



The Black Hole Universe (BHU) from a FLRW cloud

Enrique Darkcosmos.Com Gaztanaga

► To cite this version:

Enrique Darkcosmos.Com Gaztanaga. The Black Hole Universe (BHU) from a FLRW cloud. Symmetry, 2022, 14, 9, pp.1849. <10.3390/sym14091849>. <hal-03344159v5>

HAL Id: hal-03344159

<https://hal.science/hal-03344159v5>

Submitted on 5 Apr 2022

HAL is a multi-disciplinary open access archive for the deposit and dissemination of scientific research documents, whether they are published or not. The documents may come from teaching and research institutions in France or abroad, or from public or private research centers.

L'archive ouverte pluridisciplinaire **HAL**, est destinée au dépôt et à la diffusion de documents scientifiques de niveau recherche, publiés ou non, émanant des établissements d'enseignement et de recherche français ou étrangers, des laboratoires publics ou privés.



HAL Authorization

A Black Hole Universe (BHU) out of a FLRW cloud

Enrique Gaztañaga^{a,b}

^a*Institute of Space Sciences (ICE,CSIC), , Bellaterra, 08193, Barcelona, Spain*

^b*Institut d'Estudis Espacials de Catalunya (IEEC), , Barcelona, 08034, Barcelona, Spain*

Abstract

We revisit classical solutions of General Relativity (GR) where the homogeneous (FLRW) metric is a local spherical cloud of constant mass M , expanding or collapsing within a larger background. We interpret cosmic acceleration as evidence that our observed FLRW cloud is expanding inside its own Schwarzschild radius $r_S = 2GM$. We call this solution the Black Hole Universe (BHU). This model solves the horizon and structure formation problems, the two key problems of the Big Bang model, without the need of Inflation or Dark Energy. The same BHU solution can be used to understand the interior of stellar or galactic BHs. In comoving coordinates the BHU is expanding while in physical (rest frame) coordinates it is asymptotically static. We argue that such frame duality corresponds to a simple Lorentz transformation and can be further tested with current observations.

Keywords: Cosmology, Dark Energy, General Relativity, Black Holes, Dark Matter

PACS: 0000, 1111

2000 MSC: 0000, 1111

1. Introduction

The Big Bang (BB), Dark Energy (DE), Λ , inflation, DM and BHs are puzzles we don't yet understand at any fundamental level. The corresponding GR solutions, e.g. FLRW or Schwarzschild (SW) metrics, involve non physical singularities. Singularity theorems [1, 2, 3, 4], are often interpreted as an indication that a new theory of (Quantum) Gravity is needed to understand these puzzles. That a non singular version of such solutions exist is clear from direct observations. Singularities represent a simple approximation to a more complex physical solution. An example of non singular solutions are Bubble Universes. This is a domain wall that connects a region of true and false vacuum, with de Sitter (dS) space inside. These solutions are not very appealing because they have no matter or radiation anywhere, except in a surface term or bubble, required to glue the dS and SW discontinuity (e.g. see [5, 6, 7]). The BHU proposal presented here can be thought as a type of Bubble Universe with a FLRW interior (including regular matter and radiation) but no bubble or surface term.

A Schwarzschild (SW) BH metric (BH.SW) represents a singular object of mass-energy M . The BH event horizon $r_S \equiv 2GM$ prevent us from interacting with the inside (which makes BHs good candidates for DM). Physically, a singular point does not make any sense. But a physical BH can be defined, regardless of its metric, as an object of total mass-energy M with a radial size R that is smaller or equal to its SW radius r_S . The corresponding mean energy density at $R = r_S$,

$$\rho_{BH} = \frac{M}{V} = \frac{3r_S^{-2}}{8\pi G} = \frac{3M^{-2}}{32\pi G^3}. \quad (1)$$

The BH interior can not be made out of regular matter or radiation because a static non-uniform perfect fluid with mass M has

a minimal Buchdahl radius [8]:

$$R > \frac{9}{8}r_S. \quad (2)$$

But objects with mass and sizes matching r_S have been observed. What is inside a BH then? For a perfect fluid, to achieve such a high density the radial pressure inside a BH needs to be negative (see [9] and references therein).

Here we advocate for a non static but uniform solution that we call the BHU or FLRW cloud. This solution can be traced back to Oppenheimer-Snyder [10]. It corresponds to a uniform star of mass M and size R in a flat background $k = \Lambda = 0$ that collapses into a singular BH. If the collapse bounces before it becomes singular (which makes physical sense, see §4), M will be trapped inside its own Event Horizon: $R < r_S = 2GM$. We argue that such BH event horizon is a Gibbons-Hawking-York (GHY) boundary term that plays the role of Λ . This provides the BHU solution. When this solution is applied to our Universe, we discover a new interpretation for the measured Λ . Cosmic acceleration is the result of r_S and this means that our Universe becomes static in the SW (or rest) frame.

As the universe expands H tends to H_Λ which corresponds to a trapped surface $r_\Lambda = 1/H_\Lambda$, just like the event horizon of a BH. Moreover, the density of our universe in that limit is $\rho = 3H_\Lambda^2/8\pi G$ which exactly corresponds to that of a BH, in Eq.1 for $r_S = r_\Lambda$. This indicates that we live inside a BH. It also tells us that the FLRW metric is the metric inside a BH.

The idea that the universe might be generated from the inside of a BH has extensive literature (see [11, 12] and references therein) which mostly focused in dS metric with a dual role of the BH interior and an approximation for our universe. Many of the formation mechanisms involve some modifications or extensions

of GR, often motivated by quantum gravity or string theory. There are also some simple scalar field $\varphi(x)$ examples (e.g. [13]) which presented models within the scope of a classical GR and classical field theory with a false vacuum (FV) interior similar to our BH.fv solution here (see also [14]).

These models have been questioned using no-go theorems, such as that by [15], that state that no smooth solution to $\varphi(x)$ can interpolate between dS and SW space. But this is not an issue for our solution for three reasons. First, the external asymptotic space is really SW+dS or FLRW (a BH is a perturbation within a FLRW metric), where solutions do exist (e.g. [16]). Second, we do not need $\varphi(x)$ to smoothly transit between metrics: $\varphi(x)$ is trapped in a FV, which is discontinuous by nature, as shown in the Bubble Universes (e.g. see [5, 6, 7]). Finally, we do not actually need a scalar field or ρ_Λ to have a BHU solution. We just need the interior of the BH to follow a FLRW geodesic, which results in no bubble or surface terms.

Several authors before have argue that the FLRW metric could be the interior of a BH [17, 18, 19, 20, 21, 22] but these previous proposals were incomplete [23] or outside GR. They did not include a key ingredient of the BHU, that the same mass-energy M that defines the event horizon mimics a Λ term.

In §2 we present the GR field equations of a perfect fluid for homogeneous solutions: a FV and an expanding FLRW universe. We also give a brief introduction to the general case of solutions with spherical symmetry in physical SW coordinates. The FLRW solution can also be expressed in these SW coordinates. This duality is a key ingredient to interpret our BHU solution §3 and its formation §4. We end with a summary and a discussion, including observational prospects.

2. Some simple solutions

Given the Einstein-Hilbert action [24, 25, 26, 27]:

$$S = \int_{V_4} dV_4 \left[\frac{R - 2\Lambda}{16\pi G} + \mathcal{L} \right], \quad (3)$$

where $dV_4 = \sqrt{-g}d^4x$ is the invariant volume element, V_4 is the volume of the 4D spacetime manifold, $R = R^\mu_\mu = g^{\mu\nu}R_{\mu\nu}$ is the Ricci scalar curvature and \mathcal{L} the Lagrangian of the energy-matter content. We can obtain Einstein's field equations (EFE) for the metric field $g_{\mu\nu}$ from this action by requiring S to be stationary $\delta S = 0$ under arbitrary variations of the metric $\delta g^{\mu\nu}$. The solution is [28, 26, 27]:

$$G_{\mu\nu} + \Lambda g_{\mu\nu} = 8\pi G T_{\mu\nu} \equiv -\frac{16\pi G}{\sqrt{-g}} \frac{\delta(\sqrt{-g}\mathcal{L})}{\delta g^{\mu\nu}}, \quad (4)$$

where $G_{\mu\nu} \equiv R_{\mu\nu} - \frac{1}{2}g_{\mu\nu}R$ and \mathcal{L} is the matter Lagrangian. For perfect fluid in spherical coordinates:

$$T_{\mu\nu} = (\rho + p)u_\mu u_\nu + p g_{\mu\nu} \quad (5)$$

where u_ν is the 4-velocity ($u_\nu u^\nu = -1$), ρ , and p are the energy-matter density and pressure. This fluid is made of several components, each with a different equation of state $p = \omega\rho$. The case of a scalar field is presented in Appendix A.

Eq.4 requires that boundary terms vanish (e.g. see [29, 30, 27]). Otherwise, we need to add a Gibbons-Hawking-York (GHY) boundary term [31, 32, 33] to the action:

$$S = \int_{V_4} dV_4 \left[\frac{R - 2\Lambda}{16\pi G} + \mathcal{L} \right] + \frac{1}{8\pi G} \oint_{\partial V_4} d^3y \sqrt{-h} K. \quad (6)$$

where K is the trace of the extrinsic curvature at the boundary ∂V_4 and h is the induced metric. We will show explicitly in Appendix F.2 that the GHY boundary results in a Λ term when the evolution happens following a FLRW metric inside an expanding BH event horizon. To cancel the GHY term we need $r_\Lambda = r_S$. That Λ is a GHY term was propose in [34] and has also been later interpreted as a boundary entropy term by [35, 36, 37].

2.1. The FLRW metric in comoving coordinates

The flat FLRW metric in comoving coordinates $\xi^\alpha = (\tau, \chi, \theta, \delta)$, corresponds to an homogeneous and isotropic space:

$$ds^2 = f_{\alpha\beta} d\xi^\alpha d\xi^\beta = -d\tau^2 + a(\tau)^2 [d\chi^2 + \chi^2 d\Omega^2] \quad (7)$$

where we have introduced the solid angle: $d\Omega^2 = d\theta^2 + \sin^2\theta d\delta^2$. The scale factor, $a(\tau)$, describes the expansion/contraction as a function of comoving or cosmic time τ (proper time for a comoving observer). For a comoving observer, $u = 0$, the time-radial components of Eq.5 are:

$$\begin{pmatrix} T_{00} & T_{10} \\ T_{01} & T_{11} \end{pmatrix} = \begin{pmatrix} \rho(\tau) & 0 \\ 0 & p(\tau)a^2 \end{pmatrix} \quad (8)$$

and the solution to EFE in Eq.4 is then:

$$3 \left(\frac{\ddot{a}}{a} \right) = R_{\mu\nu} u^\mu u^\nu = \Lambda - 4\pi G(\rho + 3p) \quad (9)$$

$$H^2 \equiv \left(\frac{\dot{a}}{a} \right)^2 = H_0^2 [\Omega_m a^{-3} + \Omega_R a^{-4} + \Omega_\Lambda] \quad (10)$$

$$\Omega_X \equiv \frac{\rho_X}{\rho_c} ; \quad \rho_\Lambda \equiv \rho_{\text{vac}} + \frac{\Lambda}{8\pi G} \quad (11)$$

where $\rho_c \equiv \frac{3H^2}{8\pi G}$ and Ω_m (or ρ_m) represent the matter density today ($a = 1$), Ω_R is the radiation, ρ_{vac} represents vacuum energy: $\rho_{\text{vac}} = -p_{\text{vac}} = V(\varphi)$ in Eq.A.4, and $\rho_\Lambda = -p_\Lambda$ is the effective cosmological constant density. Note that Λ (the raw value) is always constant, but ρ_Λ (effective value) can change if ρ_{vac} changes. Given $\rho(\tau)$ and $p(\tau)$ we can use the above equations to find $a(\tau)$.

2.2. The FLRW metric as a Black Hole

Observations show that the expansion rate today is dominated by ρ_Λ . This indicates that the FLRW metric lives inside a trapped surface $r_\Lambda \equiv 1/H_\Lambda = (8\pi G\rho_\Lambda/3)^{-1/2}$, which behaves like the interior of a BH. To see this, consider outgoing radial null geodesic (the Event Horizon at τ , [38]):

$$r_* \equiv a\chi_* = a \int_\tau^\infty \frac{d\tau}{a(\tau)} = a \int_a^\infty \frac{d \ln a}{aH(a)} < \frac{1}{H_\Lambda} \equiv r_\Lambda \quad (12)$$

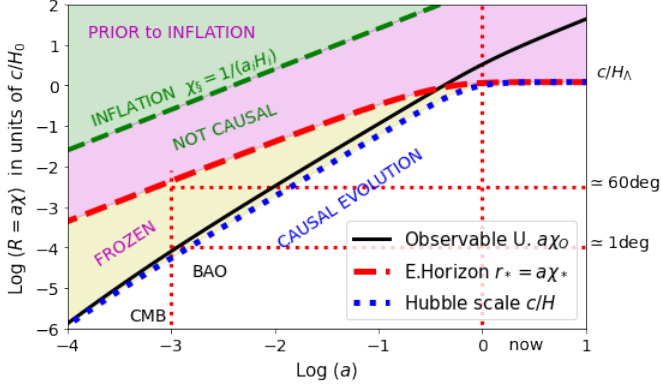


Figure 1: Physical radial coordinate $R = a(\tau)\chi$ in units of c/H_0 as a function of cosmic time a for a flat $\Omega_\Lambda = 0.75$ FLRW metric. The Hubble horizon c/H (blue dotted line), is compared to the observable universe r_o in Eq.13 (continuous line) and the FLRW Event Horizon $r_* = a\chi_*$ in Eq.12 (dashed red line), which here is smaller than the primordial causal boundary of inflation χ_\S (dashed green line). Scales larger than $a\chi_\S$ are prior to inflation. Scales larger than r_* are causally disconnected (magenta shading). Scales smaller than r_* but larger than c/H are dynamically frozen (yellow shading). At $a \simeq 1$ (now) the Hubble horizon reaches our event horizon $a\chi_* = c/H_\Lambda$. Table B.1 gives a summary of the different scales presented.

where $\chi_*(a)$ is the corresponding comoving scale. For small a the value of χ_* is fixed to a constant $\chi_* \simeq 3r_\Lambda$. Thus, the physical trapped surface radius r_* increases with time. As we approach $a \simeq 1$ the Hubble rate becomes constant and r_* freezes to a constant value $r_* = r_\Lambda$. This is shown as a red dashed line in Fig.1. No signal from inside r_* can reach outside, just like in the interior of a BH. In fact, according to Birkhoff theorem (see [39]), the metric outside should be exactly that of the BH:SW in the limit of empty outside space. So the FLRW metric is a BH:SW from the outside with $r_S = r_\Lambda$. This breaks homogeneity (on scales larger than r_Λ), but this is needed if we want causality. Homogeneity is inconsistent with a causal origin.

The causal boundary of inflation χ_\S (shown as green dashed line) corresponds to the particle horizon during inflation $\chi_\S = c/(a_i H_i)$ or the Hubble horizon $1/H_i$ when inflation begins a_i . We can in principle have that $\chi_\S > \chi_*$, as shown in the figure. But why should there be two separate causal scales? The observable universe or particle horizon is:

$$r_o = a \int_{a_e}^a \frac{d \ln a}{a H(a)} \quad (13)$$

where a_e is either $a_e = 0$ (in models without inflation) or the scale factor when inflation ends. For $\Omega_\Lambda \simeq 0.7$, the particle horizon today is $r_o \simeq 3.26c/H_0$, which is larger than r_Λ . This shows that, observers like us are trapped inside $r_* = a\chi_*$ but can probe larger scales. If we look back to the CMB maps ($a \simeq 10^3$) we can see super-horizon BAO scales (outside the Hubble scale $1/H$ at $\theta \simeq 1^\circ$ on the sky) but also scales larger than Event Horizon r_* ($\theta \simeq 60^\circ$ on the CMB sky) [40, 34, 41, 42, 43].

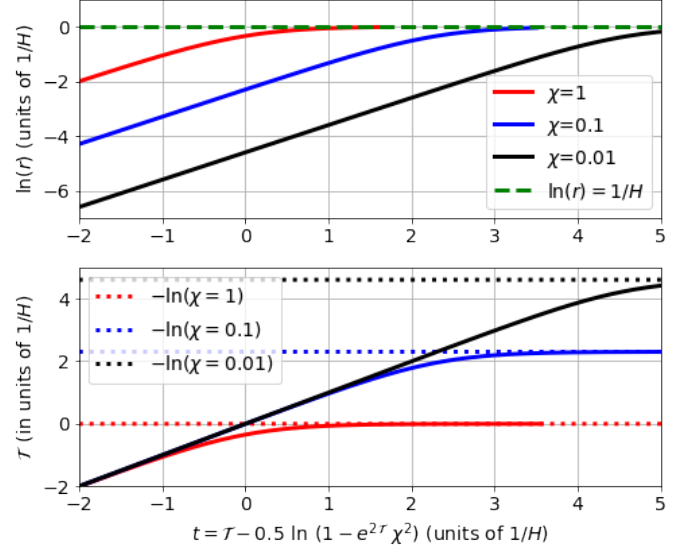


Figure 2: Logarithm of physical radius $r = a(\tau)\chi$ (top) and comoving time τ (bottom) as a function of SW time t in Eq.20 for $a(\tau) = e^{\tau H_\Lambda}$ and different values of χ . All quantities are in units of $1/H_\Lambda$. For early time or small χ : $\tau \simeq t$. A fix χ acts like an Horizon: as $t \Rightarrow \infty$ we have $\tau \Rightarrow -\ln \chi$ (dotted), which freezes inflation to: $r = a\chi \Rightarrow e^{-\ln(H_\Lambda \chi)} \chi = 1/H_\Lambda$ (dashed).

2.3. Spherical symmetry in physical coordinates

The most general shape for a metric with spherical symmetry in physical or SW coordinates (t, r, θ, δ) can be written as:

$$ds^2 = g_{\mu\nu} dx^\mu dx^\nu = -(1 + 2\Psi)dt^2 + \frac{dr^2}{1 + 2\Phi} + r^2 d\Omega^2 \quad (14)$$

where $\Psi(t, r)$ and $\Phi(t, r)$ are the two gravitational potentials. The Weyl potential Φ_W is the geometric mean of the two:

$$(1 + 2\Phi_W)^2 = (1 + 2\Phi)(1 + 2\Psi) \quad (15)$$

Ψ describes propagation of non-relativist particles and Φ_W the propagation of light. For $p = -\rho$ we have $\Psi = \Phi = \Phi_W$. Eq.14 can also be used to describe the BH:SW solution (or any other solution) as a perturbation ($2|\Phi| < 1$) around a FLRW background:

$$ds^2 \simeq -(1 + 2\Psi)dt^2 + (1 - 2\Phi)a^2 d\chi^2 + a^2 \chi^2 d\Omega^2 \quad (16)$$

where $r = a(\tau)\chi$ and $t \simeq \tau$. The same result follows from perturbing the FLRW metric in Eq.7. Appendix B reviews some known solutions with spherical symmetry.

3. The Black Hole Universe

Here we consider some additional solutions with spherical symmetry which are simple variations of the previous well known cases summarized in Table B.1.

3.1. The FLRW metric in physical coordinates

Consider a change of variables from $x^\mu = [t, r]$ to comoving coordinates $\xi^\nu = [\tau, \chi]$, where $r = a(\tau)\chi$ and angular variables

(θ, δ) remain the same. The metric $g_{\mu\nu}$ in Eq.14 transforms to $f_{\alpha\beta} = \Lambda^\mu_\alpha \Lambda^\nu_\beta g_{\mu\nu}$, with $\Lambda^\mu_\nu \equiv \frac{\partial x^\mu}{\partial \xi^\nu}$. If we use:

$$\Lambda = \begin{pmatrix} \partial_\tau t & \partial_\chi t \\ \partial_\tau r & \partial_\chi r \end{pmatrix} = \begin{pmatrix} (1+2\Phi_W)^{-1} & arH(1+2\Phi_W)^{-1} \\ rH & a \end{pmatrix} \quad (17)$$

with $2\Phi = -r^2 H^2$ and arbitrary $a(\tau)$ and Ψ , we find:

$$f_{\alpha\beta} = \Lambda^T \begin{pmatrix} -(1+2\Psi) & 0 \\ 0 & (1+2\Phi)^{-1} \end{pmatrix} \Lambda = \begin{pmatrix} -1 & 0 \\ 0 & a^2 \end{pmatrix} \quad (18)$$

In other words, these two metrics are the same:

$$-(1+2\Psi)dt^2 + \frac{dr^2}{1-r^2H^2} = -d\tau^2 + a^2 d\chi^2 \quad (19)$$

The dSE metric in Eq.B.9 with $2\Phi = -r^2 H^2$ corresponds to the FLRW metric with $H(t, r) = H(\tau)$: this is a hypersphere of radius r_H that tends to r_Λ (see Appendix C). This frame duality can be understood as a Lorentz contraction $\gamma = 1/\sqrt{1-u^2}$ where the velocity u is given by the Hubble-Lemaître law: $u = Hr$ (which results from $r = a\chi$). An observer in the SW frame, not moving with the fluid, sees the moving fluid element $ad\chi$ contracted by the Lorentz factor γ : $ad\chi \Rightarrow \gamma dr$. For constant H , the FLRW metric corresponds the interior of a BH with constant density in Eq.B.2. A Lorentz factor γ also explains $d\tau = \gamma^{-1} dt$ as time dilation. Given $a(\tau)$, we can find Ψ and $\tau = \tau(t, r)$. For $a(\tau) = e^{\tau H_\Lambda}$ we have $2\Psi = 2\Phi = -r^2 H_\Lambda^2$ and (see [44, 45]):

$$t = t(\tau, \chi) = \tau - \frac{1}{2H_\Lambda} \ln [1 - \chi^2/\chi_H^2], \quad (20)$$

where $\chi_H = \frac{1}{aH_\Lambda}$ and reproduces dS metric (see [46] for some additional discussion). In comoving coordinates the metric is inflating exponentially: $a = e^{\tau H_\Lambda}$, while in physical coordinates it is static. Fig.2 illustrates how this is possible and shows how $\tau = \tau(t, r)$ freezes to a constant as $t \rightarrow \infty$ (this is because χ_H shrinks to zero). Note also how $\partial_\tau t = (1+2\Phi_W)^{-1}$ in Eq.17 for $2\Phi_W = -r^2 H^2$ is the generalization of Eq.20 for $\dot{H} \neq 0$.

3.2. FLRW cloud & Black Hole Universe (BH.u)

In Appendix D we present the simplest case of a non singular BH solution (BH.fv) with a FV inside and without Bubble. This solution can be view as limiting case of a solution where we have matter $\rho_m = \rho_m(t, r)$ and radiation $\rho_R = \rho_R(t, r)$ inside some radius R and empty space outside:

$$\rho(t, r) = \begin{cases} 0 & \text{for } r > R \\ \Delta + \rho_m + \rho_R & \text{for } r < R \end{cases} \quad (21)$$

For uniform density inside this should reproduce the FLRW solution for $r < R$ and the SW solution for $r > R$. This follows from Gauss law (or the corollary to Birkhoff's theorem [47]) where each sphere $r < R$ collapses independent of what is outside $r > R$. To see this more explicitly for the interior solution, we use the dSE notation in EqB.9: $2\Phi(t, r) \equiv -r^2 H^2(t, r) \equiv -r^2/r_H^2$, so that:

$$2\Phi(t, r) = \begin{cases} -r_S/r & \text{for } r > R \\ -r^2 H^2 & \text{for } r < R \end{cases} \quad (22)$$

At the junction $r = R$, we find that:

$$R = [r_H^2 r_S]^{1/3}, \quad (23)$$

For a regular star $R > r_S$ so the expansion is subluminal $R < r_H$. Our Universe has $R > r_H$ (we observe super-horizon scales in the CMB) which using Eq.23 requires $R < r_S$: i.e. we are inside our own BH! For $r < R$ we can change variables as in Eq.17-19. In the comoving frame of Eq.19, from every point inside de BHU, comoving observers will have the illusion of an homogeneous and isotropic space-time around them, with a fixed Hubble-Lemaître expansion $H(\tau)$. This converts dSE metric into FLRW metric. So the solution is $H(t, r) = H(\tau)$ and $R(\tau) = [r_S/H^2(\tau)]^{1/3}$. Given $\rho(\tau)$ and $p(\tau)$ in the interior we can use Eq.10 to find $H(\tau)$ and $R(\tau)$:

$$H^2(\tau) = \frac{8\pi G}{3} \rho(\tau) = \frac{r_S}{R^3(\tau)} \quad (24)$$

This corresponds to a homogeneous FLRW cloud of fix mass-energy $M = r_S/2G$ confined inside $R(\tau)$. When $R > r_S$ we call this a FLRW cloud and when $R < r_S$ this is a BH Universe (BH.u of type BH.u). The comoving radius χ_* corresponding to R is $\chi_*(\tau) \equiv R(\tau)/a(\tau)$. We can see how R can be related with a freefall geodesic radial shell:

$$\frac{dR}{d\tau} = a \frac{d\chi_*}{d\tau} + \chi_* \frac{da}{d\tau} = V_0 + HR = V_0 + (r_S/R)^{1/2} \quad (25)$$

where $V_0 \equiv a\dot{\chi}_*$. For a time-like geodesic of constant χ_* ($d\chi = 0$) we have $V_0 = 0$. For a null-like geodesic ($ad\chi = d\tau$): $V_0 = 1$. The later case corresponds to $R = r_*$ in Eq.12 from which we can immediately see that $r_S = r_\Lambda$ like in the BH.fv solution of Eq.D.2. So even when $\Lambda = \Delta = 0$, the mass M inside R generates $r_\Lambda = r_S$. We will come back to this point in Appendix F.2. We can integrate Eq.25 to find $R(\tau)$, for a fix V_0 and r_S , regardless of $\rho(\tau)$. This shows that a solution for $R(\tau)$ exist for any content inside R . To complete the solution, i.e. to find Ψ and $\tau = \tau(t, r)$, we need to solve Eq.17 with $2\Phi = -r^2 H^2(\tau)$. For $H(\tau) = H_\Lambda$ the solution is $\Psi = \Phi$ and Eq.20. The FLRW metric with $H = H_\Lambda$ becomes dS metric in Eq.B.6 as in the BH.fv solution Eq.D.2. Such solutions are illustrated in Fig.B.6.

3.3. A frozen BH internal layer

Note how Eq.23 indicates that there is a region with matter outside the Hubble horizon $R > r > r_H$. The region increases during collapse inside a BH and re enters the Hubble horizon as it expands. This is a potential source of frozen perturbations, which acts very much like Cosmic Inflation if there is bouncing solution (see §4)). This is illustrated in Fig.3 (see also Fig.1) and will be further discussed in §4.2

4. The formation of the BHU

How does a BH or our cosmic expansion evolve into the solution of Eq.22? This is an important question. It is not enough to find a solution to EFE. We need to make sure that

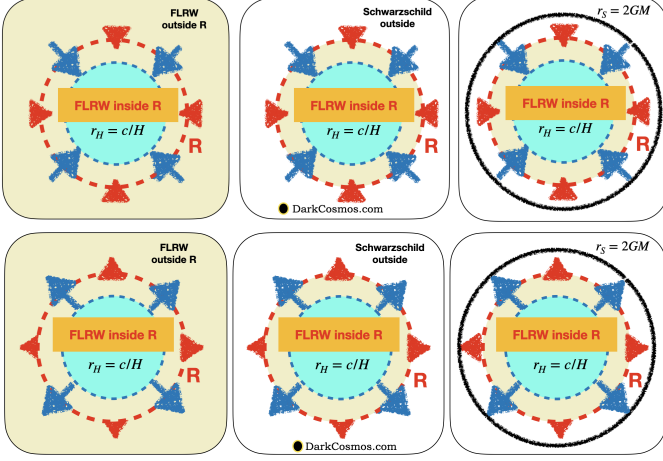


Figure 3: The FLRW metric can be used to model an infinite universe (left), collapsing (top) or expanding (bottom), and a cloud of finite mass M and size $R(\tau)$ (red circle) in empty space (middle) or inside its SW radius $r_S = 2GM$ (right). The Hubble Horizon $r_H = H^{-1}$ (blue circle, relative to the center) moves faster than R , so that perturbations become super-horizon during collapse and re-enter during expansion, solving the horizon problem without Inflation.

such a configuration can be achieved in a causal way. A good example of this problem is the infinite FLRW solution. The Hubble rate is the same everywhere, not matter how far, and this is not causally possible [40, 34]. Cosmic Inflation alleviates this problem, but does not solve it.

We propose here two possible BHU formation scenarios: one that happens during a rapid expansion (or explosion) and a version that happens during the collapse. Both can be applied to a small object, like a star, or a large object, like our Universe. The main difference is that for the larger object the density corresponding to r_S is very low (few atoms per cubic meter) and we can assume a dust ($p = 0$) fluid. This is not the case for small object, like a star. But stars do eventually collapse and explode. Here we focus in formation scenario during collapse which we consider more appealing as it does not require a FV, inflation or DE. In Appendix G we present the expanding scenario.

4.1. FLRW Cloud collapse

Consider a large cloud dominated by dust or CDM (ρ_m with $p = 0$) with radius R and mass M , surrounded by a region of empty space. The detail composition is not important now, but could play some role later on. This is a good approximation for our Universe with $M \simeq 5 \times 10^{22} M_\odot$ which corresponds to the mass inside our FLRW event horizon r_Λ . The resulting BH density is very low, $\rho_{BH} = 3r_S^{-2}/8\pi G = \rho_\Lambda$, which is 25% lower than the critical density today $\rho = 3H_0^2/8\pi G$ (a few protons per cubic meter).

Gravity will make such dust cloud collapse following a freefall timelike geodesic of Eq.22 with R given by Eq.F.10: $R = (r_H^2 r_S)^{1/3}$. As there is no pressure support, it will eventually collapse into a BH when $R = r_S = r_H = 2GM$. The event horizon does not stop the collapse as it only prevents outgoing null geodesics, but it welcomes incoming events. Because of the Equivalence Principle, spherical free falling shells do not feel

the BH gravity pull. So the collapse continues freefall inside the BH as illustrated in the left half of Fig.4 where the junction $R = (r_H^2 r_S)^{1/3}$ remains valid.

The density increases as $\rho \sim \Delta\tau^{-2}$, where $\Delta\tau$ is the time remaining to reach $R = 0$. As the density inside gets larger it will resist further collapse. The density eventually reaches the nuclear atomic density (of a neutron star) which produces a bounce or explosion. This is similar to a supernova explosion or a hot Big Bang. The expansion follows the standard cosmic evolution (nucleosynthesis, CMB decoupling and so on). During radiation domination the junction follows the null geodesic rather the timelike geodesic. The resulting fluid cools down as it expands. Finally the expansion halts as it reaches back to $R = r_S$.

As detailed in Appendix F.2 the evolution inside a BH event horizon induces a Λ term in the EFE even when there is no Λ term to start with. This provides a fundamental interpretation to the observed Λ as causal boundary [40, 34, 48].

The bottom panel of Fig.4 shows an actual numerical calculation for the formation of our Universe. During collapse, the boundary R is fixed in comoving coordinates and follows $R = [r_H^2 r_S]^{1/3}$, where we have fixed $r_S = 2GM$ to its observed value today $r_S = \Omega_\Lambda^{-1/2}/H_0$ with $\Omega_\Lambda \simeq 0.75$ and r_H is just given by Eq.10 with $\Omega_m \simeq 0.25$ and $\Omega_\Lambda = 0$. After the Big Bang, R follows a null geodesic $ad\chi = d\tau$ (red dashed line) with $H(\tau)$ given by $\Omega_\Lambda \simeq 0.75$ and $\Omega_m \simeq 0.25$. The Big Bang happened $\tau \simeq H_0^{-1} \simeq 14\text{Gyrs}$ ago and our Universe collapsed into a BH about 25Gyrs ago.

4.2. Is Cosmic Inflation needed?

Inflation [49, 50, 51, 52] is a key ingredient in the standard cosmological model. For a review see [53, 54] and also Appendix G. It solves several problems, the most relevant here are: 1) the horizon problem 2) the source of LSS 3) the flatness problem 4) the monopole problem. The horizon and LSS problems rise because much of the LSS that we observed today, e.g. BAO in CMB maps, was outside the Hubble horizon r_H at the time of light emission and therefore could not have had a causal origin. The idea of inflation is that during the very first instances of the hot Big Bang expansion the Universe became dominated by some FV or DE which produced a dS expansion phase. Such exponential expansion solves all the above problems. After expanding by a factor e^{60} , Inflation leaves the universe empty and we need a mechanism to stop Inflation and to create the matter and radiation that we observe today. This is called re-heating. These require fine-tuning and free parameters that we do not understand at a fundamental. Inflation is not directly observable or testable, because it occurred when the Universe was opaque and at energies ($> 10^{15}\text{GeV}$) that are out of reach in particle accelerators [54].

As detailed in §3.3 and Fig.3, a large fraction of the mass M that collapsed into our BHU is outside r_H , specially close to the Big Bang phase, as $R = [r_H^2 r_S]^{1/3}$ (see Fig.4). This clearly solves the horizon problem. Perturbations can be generated during the collapse and exit the horizon. Such super-horizon perturbations can be the source of LSS structures when they re-enter r_H during expansion. Long before Inflation was invented,

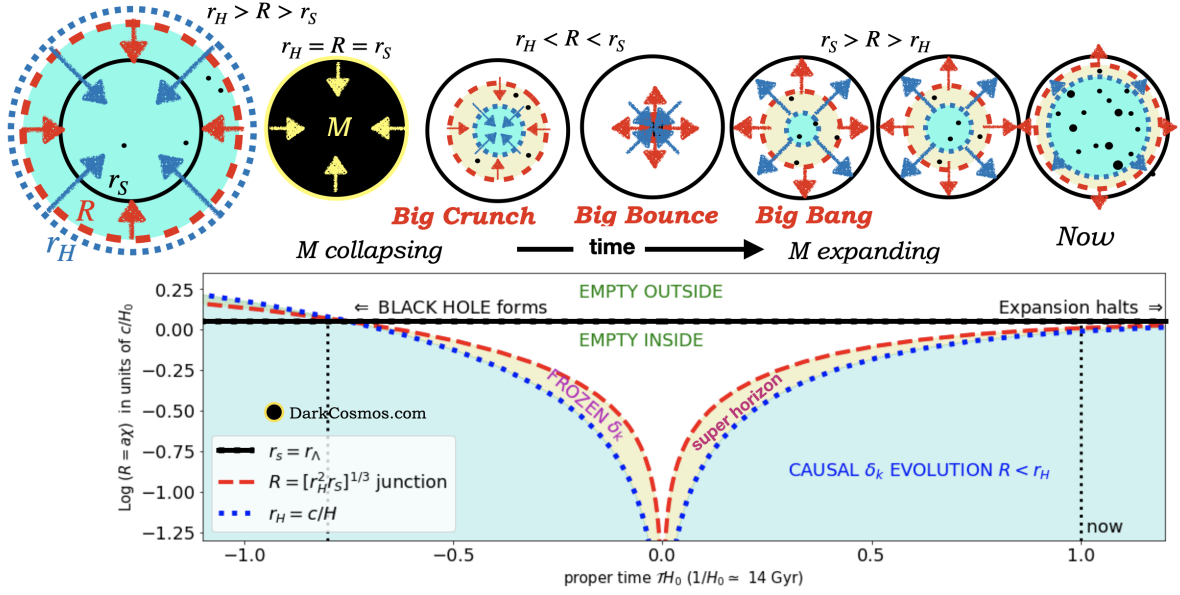


Figure 4: Illustration of the formation of a BHU. A cloud of radius R and mass M collapses under gravity. When it reaches $R = r_S = 2GM$ it becomes a BH. The collapse proceeds inside the BH until it bounces producing an expansion (the hot Big Bang). The event horizon r_S behaves like a cosmological constant with $\Lambda = 3/r_S^2$ so that the expansion freezes before it reaches back to $r_S = r_\Lambda$. The bottom panels shows a numerical calculation for $\Omega_\Lambda = 0.75$ with $R = [r_H^2 r_S]^{1/3}$. Structure in-between R and r_H is frozen and seeds structure formation in our Universe, which could include smaller BHUs, CMB, stars and galaxies.

Harrison [55], Zel'dovich [56] and Peebles [57] proposed that gravitational instability of regular matter alone can generate a scale invariant spectrum of fluctuations, very similar to that predicted in models of Inflation. This means that both models (Inflation or the BHU) can make similar predictions.

Our results can be extended to a FLRW cloud with $k \neq 0$. We can reproduce the derivation that lead to Eq.F.10 if we define $r_H^{-2} \equiv H^2 + k/a^2 = \frac{8\pi G}{3}\rho$ so this does not change our BHU model or interpretation. A time-like geodesic of constant comoving radius χ_* contains the same constant mass M also for $k \neq 0$. The flatness problem solved by inflation, is only a problem if we allow for a non flat topology in the FLRW metric. But why choose a topology for empty space? The so call flatness problem, that is solved by Inflation, is only a problem if the Big Bang singularity creates curvature. The same can be argued about Λ . The field equations of GR are local and they do not change k or Λ because these are global topological quantities which are not altered by the presence of matter. So any choice other than $k = \Lambda = 0$ would require some justification that is outside GR. In our analysis we assumed the most simple topology, that of empty space with $k = \Lambda = 0$. In the BHU model the singularity is avoided at GeV, well before Quantum Gravity effects (10^{19} GeV), so we do not expect monopoles, a global curvature or Λ .

5. Discussion & Conclusion

The solution in Eq.22 corresponds to what we call here a FLRW cloud for $R > r_S$. That such FLRW sphere solutions exist is well known [10, 47]. The cloud can collapse to become a BHU ($R < r_S$). This BH is not static inside, which explains how we avoid the constrain $R > 9r_S/8$ in Eq.2. We have studied the

junction conditions (see Appendix F) to show the join manifold (FLRW+SW) is also a solution to EFE and there are no surface terms. As it happens with the SW metric, the exterior metric of the BHU could also be FLRW (e.g. see [58] and Eq.16). So in the BHU we have two nested FLRW metrics. This is illustrated in bottom right of Fig.B.6. We can have smaller BHs inside larger BHs or smaller FLRW metrics inside larger FLRW universes. Mathematically this looks like a Matryoshka (or nesting) doll [17] or a fractal structure [22]. But physically, each BH has a different mass and therefore different physical properties and internal structure.

Another issue, which we address in §4 and Appendix G, is how such physical BHU solutions can be achieved (e.g. astrophysical and primordial BH formation) and if they can have a causal origin. We propose two possible BHU formation scenarios: one that involves FV and can only happen during a rapid expansion (or explosion) and a version that originates in a stellar collapse. Both can be applied to a small object, like a star, or a large object, like our Universe. We have focused in the collapsing case which can result in a BHU without DE or FV. The expanding scenario requires a FV and is presented in Appendix G. The collapsing scenario is illustrated in Fig.4.

We conjecture here that the bounce happens because of the Pauli Exclusion Principle in Quantum Mechanics which prevents fermions to occupy the same quantum state. This is the same physics that explains core collapse supernovae. This Big Bounce is the beginning of a non-singular Big Bang expansion. The BH event horizon is the causal boundary to our Universe expansion and produces the observed cosmic acceleration, that we interpret as DE (see also [48, 59]).

As pointed out in the introduction, that the universe might be generated from the inside of a BH has a long and interesting

history. Knutsen [23] argued that p and ρ in the homogeneous FLRW solution are only a function of comoving time and can not change at $r = r_S$ to become zero in the exterior. But homogeneity is the illusion of the comoving observer inside r_S . The FLRW metric is trapped inside r_* (Eq.12), and is then equivalent to a spherically symmetric metric of Eq.19.

The FLRW homogeneous solution seems to have larger symmetry (more killing vectors) than the FLRW cloud. This is certainly the case for $R > r_S$: a comoving observer would see the Hubble law of Eq.10 from anywhere inside but the measured background density would not be isotropic unless you are at the center. But this is not the case when we have Λ or, equivalently, when we are inside a BH. This is apparent in deSitter metric, which can be expressed as a homogeneous expanding FLRW metric or as a (inhomogeneous) static hypersphere of Eq.B.6. So the killing vector counting must be the same, as it corresponds to the same solution. For $R < r_S$, a co-moving observer anywhere inside such a local FLRW cloud has no way to distinguish it from an infinite FLRW universe. We can understand this curious behavior in the dual frame by considering radial null events ($ds^2 = 0$) connecting $(0, r_0)$ with (t, r) in deSitter metric, which follow Eq.B.7. It takes $t = \infty$ to reach $r = r_\Lambda$ from any point inside, no matter where you are. This agrees with Eq.12.

The BHU can be falsified if we measure that the DE equation of state is $\omega \neq -1$. This would indicate that cosmic acceleration is not caused a the BH causal event horizon r_S . We can actually observe scales that are larger than r_S . At the time of CMB last scattering, r_S corresponds to an angle $\theta = \chi_*/\chi_o \lesssim 1 \text{ rad} \simeq 60 \text{ deg}$. Such super-horizon scales could be related to the so-called CMB anomalies, deviations with respect to inflationary predictions from Λ CDM (see [34, 41, 42, 60] and references therein), or the apparent tensions in measurements from different cosmic scales or times [61].

The BHU model allows a Perfect Cosmological Principle, the one advocated by Einstein (when he introduced Λ) and the Steady State Cosmology [62, 63, 64]. But there is no need for ad hoc matter creation (the C-field) to explain the observed cosmic expansion. The frame duality in Eq.19 explains how we can have at the same time an expanding universe in comoving coordinates (as observed by the Hubble-Lemaître law) and an asymptotically static BHU in the outside SW frame.

Acknowledgements

I want to thank Marco Bruni, Robert Caldwell, Ramin G. Daghigh, Alberto Diez-Tejedor and Angela Olinto, for their feedback. This work has been supported by spanish MINECO grants PGC2018-102021-B-100 and EU grants LACEGAL 734374 and EWC 776247 with ERDF funds. IEEC is funded by the CERCA program of the Generalitat de Catalunya.

Appendix A. Scalar field in curved space-time

Consider a minimally coupled scalar field $\varphi = \varphi(x_\alpha)$ with:

$$\mathcal{L} \equiv K - V = -\frac{1}{2}\partial_\alpha\varphi\partial^\alpha\varphi - V(\varphi) \quad (\text{A.1})$$

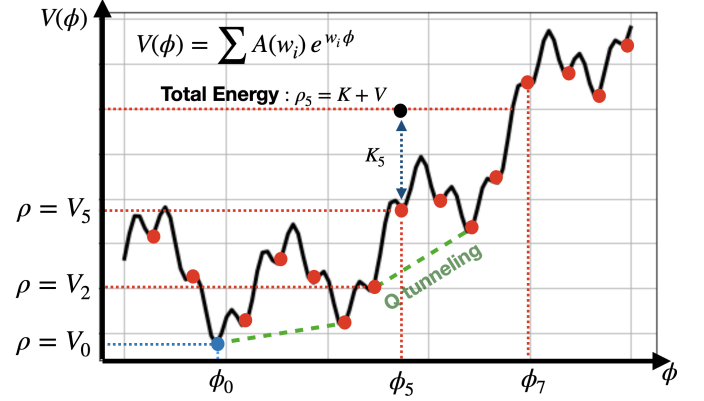


Figure A.5: The potential $V(\phi)$, of a classical scalar field $\phi(x)$, made of the superposition of plane waves. A configuration with total energy: $\rho_5 = K_5 + V_5$ (black dot at ϕ_5) can loose its kinetic energy K_5 during expansion (e.g. a supernova explosion or a expanding background) due to Hubble damping and relax into one of the static ($K = 0$) ground state (or FV) $\rho_5 = V_5 \equiv V(\phi_5)$ (red dots). This can generate a Black Hole (BH.fv) and regular matter from reheating. Each FV has an energy excess $\Delta_i \equiv V_i - V_0$ over the true vacuum at V_0 (blue dot). Quantum tunneling (dashed lines) could allow ϕ to jump between FV, resulting in BH evaporation and new matter/radiation.

The Lagrange equations are: $\bar{\nabla}^2\varphi = \partial V/\partial\varphi$. We can estimate $T_{\mu\nu}(\varphi)$ from its definition in Eq.4 to find [26]:

$$T_{\mu\nu}(\varphi) = \partial_\mu\varphi\partial_\nu\varphi + g_{\mu\nu}(K - V) \quad (\text{A.2})$$

comparing to Eq.5:

$$\rho = K + V \quad ; \quad p = |K| - V \quad (\text{A.3})$$

In general we can have $p_{\parallel} \neq p_{\perp}$ for non canonical scalar fields (see Eq.5 in [65] for further details). The stable solution corresponds to $p = -\rho \equiv -\rho_{vac}$:

$$\bar{\nabla}^2\varphi = \partial V/\partial\varphi = 0 \quad ; \quad \rho \equiv \rho_{vac} = -p = V(\varphi) = V_i \quad (\text{A.4})$$

where φ is trapped in the true minimum V_0 or some false vacuum (FV) state $V_i = V_0 + \Delta$. The situation is illustrated in Fig.A.5. The solution to Eq.4 for constant $\rho = -p = V_i$ (without matter or radiation) for a general metric with spherical symmetry in physical coordinates (i.e. Eq.14) is given by dS metric in Eq.B.6 with $H_\Lambda^2 \equiv 8\pi G\rho_\Lambda/3$ where $\rho_\Lambda = V_i + \Lambda/8\pi G$. This metric is static which indicates that the vacuum solution is in equilibrium.

Appendix B. Some well known solutions

Solutions to EFE for Eq.14 are well known, e.g. see Eq.(7.51) in [27]. For a static perfect fluid BH with arbitrary $\rho(r)$ inside r_S and empty space ($\Lambda = 0$) outside, we have $G_0^0 = -8\pi G\rho(r)$. This can be solved using $m(r)$:

$$\Phi(r) = -\frac{Gm(r)}{r} = -\frac{G}{r} \int_0^r \rho(r) 4\pi r^2 dr \quad (\text{B.1})$$

so the interior $r < r_S$ of a BH has [66]:

$$\Phi(r) = \begin{cases} -GM/r & \text{for } \rho(r) = M \delta_D(r) \\ -\frac{1}{2}(r/r_0)^2 & \text{for } \rho(r) = \rho_0 \equiv \frac{3}{8\pi r_0^2} \end{cases} \quad (\text{B.2})$$

$\Psi(r)$ depends on G_1^1 and $p(r)$. For $p = -\rho$ we have $G_0^0 = G_1^1$ and the general solution with $\Lambda \neq 0$ is:

$$\Phi = \Psi = -\frac{Gm(r)}{r} - \frac{\Lambda r^2}{6} \quad (\text{B.3})$$

The remaining EFE in Eq.4 are $G_2^2 = G_3^3$ and correspond to energy conservation $\nabla_\mu T_\nu^\mu = 0$. For a comoving observer $u = 0$ in a perfect fluid of Eq.5:

$$\partial_t \rho = -\frac{\rho + p}{1 + 2\Phi} \partial_t \Phi. \quad ; \quad \partial_r p = \frac{\rho + p}{1 + 2\Phi} \partial_r \Psi \quad (\text{B.4})$$

Note how $\rho = -p$ results in constant ρ and p in time and everywhere, but with a discontinuity at $2\Phi = 2\Psi = -1$. This means that ρ and p could be constant but different in both sides of $2\Phi = 2\Psi = -1$. This will be addressed with the study of junction conditions in Appendix F).

Empty space ($\rho = p = \rho_\Lambda = 0$) in Eq.B.3 results in the BH.SW metric:

$$2\Phi = 2\Psi = -2GM/r \equiv -r_S/r \quad (\text{B.5})$$

There is a trapped surface at $r = r_S$ ($2\Phi = -1$). Outgoing radial null geodesics cannot leave the interior of r_S , while incoming ones can cross inside. The solution to Eq.B.3 for $\rho = p = M = 0$, but $\rho_\Lambda \neq 0$ results in deSitter (dS) metric:

$$2\Phi = 2\Psi = -r^2/r_\Lambda^2 \equiv -r^2 H_\Lambda^2 = -r^2 8\pi G \rho_\Lambda / 3 \quad (\text{B.6})$$

where ρ_Λ is the effective density: $\rho_\Lambda = \Lambda/(8\pi G) + V(\varphi)$. We can immediately see that this solution is the same as the interior of a BH with constant density in Eq.B.2 with $\rho_0 = \rho_\Lambda$.

dS metric corresponds to the surface of a hypersphere of radius r_Λ in a flat spacetime with an extra spatial dimension (see Appendix C). This has a constant positive Ricci curvature $R = 4\Lambda$ and a finite volume inside r_Λ . As in the BH.SW metric, dS metric also has a trapped surface at $r = r_\Lambda$ ($2\Phi = -1$). Radial null events ($ds^2 = 0$) connecting $(0, r_0)$ with (t, r) follow:

$$r = r_\Lambda \frac{r_\Lambda + r_0 - (r_\Lambda - r_0)e^{-2t/r_\Lambda}}{r_\Lambda + r_0 + (r_\Lambda - r_0)e^{-2t/r_\Lambda}} \quad (\text{B.7})$$

so that it takes $t = \infty$ to reach $r = r_\Lambda$ from any point inside. The BH.SW metric is singular at $r = 0$, while dS is singular at $r = \infty$. But note that this singularity can not be reached from the inside because of the trapped surface at r_Λ in Eq.B.7. The inside observer is trapped, like in the FLRW case. Both metrics are equivalent for $H = H_\Lambda$ (see [44, 46]) which explains why the dS metric reproduces primordial inflation in comoving coordinates. For M and ρ_Λ constant, the solution to Eq.B.3 is:

$$2\Phi = 2\Psi = -r^2 H_\Lambda^2 - r_S/r, \quad (\text{B.8})$$

which corresponds to dS-SW (dSW) metric, a BH.SW within a dS background. Solution of a BH inside a FLRW metric also exist (e.g. see [58]). Here we will show that GR solutions also exist for a FLRW inside a BH (or inside a larger FLRW metric).

We also consider a generalization of dS metric, which we call dS extension (dSE), which is just a recast of the general case:

$$2\Phi(t, r) \equiv -r^2 H^2(t, r) \equiv -r^2 / r_H^2 \quad (\text{B.9})$$

Table B.1 shows a summary of notation and metrics considered in this paper.

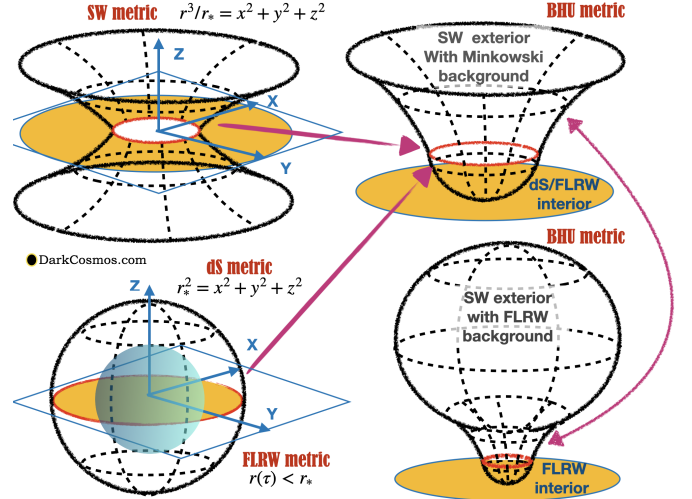


Figure B.6: Spatial representation of $ds^2 = (1 + 2\Phi)^{-1} dr^2 + r^2 d\theta^2$ 2D metric embedded in 3D flat space for: deSitter (dS, bottom left, $2\Phi = -r^2/r_\Lambda^2$), FLRW ($r(\tau) < r_*$, blue sphere inside dS), Schwarzschild (SW, top left, $2\Phi = -r_s/r$) and two versions of the combined BHU metrics. Yellow region shows the projection coverage in the (x, y) plane. In the top right figure we show a BHU with dS (or FLRW) interior and SW metric exterior joint at the Event Horizon $r_* = 2GM = 1/H_\Lambda$ (red circles). The BHU solution has in general two nested FLRW metrics join by SW metric (bottom right). see Appendix C for a more detailed explanation.

Appendix C. Geometrical representations

To visualize the BHU metric in a 2D plot we consider the most general shape for a spherically symmetric metric in 2D space (x, y) embedded in 3D flat space (x, y, z) (see also §7.1.3 in [27]). In polar coordinates (r, θ) with $r^2 = x^2 + y^2$ and $\tan \theta = x/y$ we have:

$$ds^2 = \frac{dr^2}{1 + 2\Phi} + r^2 d\theta^2 \quad (\text{C.1})$$

In 3D space we just have one additional angle, δ , in Eq.14, but the radial part is the same. The case $\Phi = 0$ corresponds to flat space: $ds^2 = dx^2 + dy^2$. The simplest case with curvature can be represented by a 2D sphere (S2) embedded in 3D flat space using an extra dimension z :

$$ds^2 = dx^2 + dy^2 + dz^2 \quad ; \quad x^2 + y^2 + z^2 = r_*^2 \quad (\text{C.2})$$

This metric is flat in 3D coordinates, but constraint to r_* , which is the radius of the sphere and the curvature within the 2D surface of S2. We can replace z by r using: $z^2 = r_*^2 - r^2$ to find:

$$ds^2 = dx^2 + dy^2 + dz^2 = \frac{dr^2}{1 - r^2/r_*^2} + r^2 d\theta^2 \quad (\text{C.3})$$

so that $2\Phi = -r^2/r_*^2$ just like in the dS metric of Eq.B.6 for $r_* = r_\Lambda$. It tell us that dS space corresponds to being in the flat surface of a sphere (like us in Earth). This is illustrated in the bottom left of Fig.B.6. Note how (r, θ) are coordinates in the (x, y) plane. The S2 space is trapped or bounded by $r < r_*$ (yellow region). The metric changes signature (becomes imaginary) for $r > r_*$: this region can't be reached (white

Table B.1: Some notation used in this paper.

Notation	name	comment
$r_\Lambda = 1/H_\Lambda$	deSitter (dS) Event Horizon	$3H_\Lambda^2 = 8\pi G\rho_\Lambda$, Eq.B.6
$-2\Phi = r^2 H_\Lambda^2$	dS metric Eq.B.6	static, inside BH.fv
$r_S = 2GM$	BH Event Horizon	$\rho_{BH}(r_\Lambda) = \rho_\Lambda$, Eq.1
$-2\Phi = r_S/r$	Schwarzschild (SW) metric	BH.SW, outside BHU, Eq.B.5
$-2\Phi = r_S/r + r^2 H_\Lambda^2$	dSW = dS-SW	static, outside BHU, Eq.B.8
$-2\Phi = \begin{cases} r_S/r & \text{for } r > r_S \\ r^2 H_\Lambda^2 & \text{for } r < r_S \end{cases}$	False Vacuum or BH.fv	frozen BHU in Eq.D.2
$r_* = a\chi_*(\tau) = a \int_\tau^\infty \frac{d\tau}{a(\tau)}$	FLRW Event Horizon	Outgoing null geodesic Eq.12
$r_H = 1/H$	Hubble Horizon	$r > r_H$ frozen Fig.1
$-2\Phi = r^2 H^2$	dSE= dS Extension Eq.B.9	FLRW or BH.u interior Eq.19
$R = [r_H^2 r_S]^{1/3}$	BHU Junction Eq.23, Eq.F.10	Null geodesic: $R = r_*$ Eq.F.22
$-2\Phi = \begin{cases} r_S/r & \text{for } r > R \\ r^2 H^2 & \text{for } r < R \end{cases}$	FLRW cloud for $R > r_S$	BH.u for $R < r_S$, Eq.22
$r_o = a\chi_o = a \int_0^\tau \frac{d\tau}{a(\tau)}$	Observable Universe Eq.13	Particle Horizon today $r_o > r_\Lambda$
$r_\S = a(\tau)\chi_\S = a(\tau)\chi_*$	Causal Boundary Eq.F.4	for Inflation: $\chi_\S = \chi_* = (a_i H_i)^{-1}$

region). The case $r = r_*$ (red circles) corresponds to the Event Horizon at $2\Phi = -1$.

The Newtonian interpretation of $2\Phi = -r^2/r_*^2$ is that this is caused by a centrifugal force, like that in the orbit of a satellite. Even when there is no matter, the curvature (or boundary) is interpreted as a repulsive gravitational force that causes acceleration.

The FLRW metric (or dSE metric in Eq.19) correspond to a smaller sphere S2 (inside dS sphere) with an expanding radius $r_H(\tau)$ that tends asymptotically to $r_\Lambda = 1/H_\Lambda$ (see Eq.19):

$$ds^2 = dx^2 + dy^2 + dz^2 \quad ; \quad x^2 + y^2 + z^2 = r_H^2(\tau) \quad (\text{C.4})$$

So it has the same topology and Event Horizon or trapped surface (red circle) as dS metric. It is represented in Fig.B.6 by a blue sphere inside dS sphere in the bottom left corner. This illustrates how it is possible that each observer inside sees an homogeneous space even when the sphere is centered around a given position.

The next simplest case can be represent by a static radius that increases with r , i.e. : $x^2 + y^2 + z^2 = r^3/r_*$. We can replace z by r using: $z^2 = r^3/r_* - r^2$ to find:

$$ds^2 = dx^2 + dy^2 + dz^2 = \frac{dr^2}{1 - r_*/r} + r^2 d\theta^2 \quad (\text{C.5})$$

so that $2\Phi = -r_*/r$ just like in the SW metric of Eq.B.5 for $r_* = 2GM$. This is illustrated in the top left of Fig.B.6. The case $r = r_*$ (red circle) corresponds to the Event Horizon at $2\Phi = -1$. The Newtonian interpretation for $2\Phi = -r_*/r$ is the inverse square law for a point mass M : $r_* = 2GM$.

The SW space is bounded by $r > r_*$ (yellow region). The metric changes signature (becomes imaginary) for $r < r_*$ and this region can not be reached. This coverage is complementary to dS or FLRW metric which only cover the inner region. We can match the dS and SW metrics at $r = r_*$ to cover the full (x, y) plane as in the BHU metric. Physically this corresponds to a balance between the centrifugal force, represented by dS potential $2\Phi = -r^2/r_*$, and the SW inverse square law, $2\Phi =$

$-r_*/r$, like what happens in the circular Keplerian orbits. This matching is the junction in Eq.F.10 which corresponds to a causal boundary. This can also be seen as a Lorentz contraction $\gamma = 1/\sqrt{1 - u^2}$ where the velocity u is given by the Hubble-Lemaître law: $u = Hr$. The time duality between the FLRW and SW frame can also be interpreted as a time dilation, see Eq.19.

This BHU metric is shown in the top right of Fig.B.6, which is asymptotically Minkowski. The dS metric is the limiting case of FLRW metric and SW metric is a perturbation over FLRW metric. So more generally, the BHU is a combination of 2 FLRW metrics join by a SW metric. The junction happens at the effective value of $r_* = r_\Lambda = 2GM$ corresponding to the inner FLRW ρ_Λ (which we denote as ρ_{Λ_-}). If the outer FLRW has $\rho_{\Lambda_+} \neq 0$, then the SW hyperbolic surface will close as another S2 sphere (bottom right).

Appendix D. False Vacuum Black Hole (BH.fv)

Eq.B.5 and Eq.B.6 are the simplest solutions to EFE. They correspond to some form of empty space. The simplest modeling of physical BH interior is a combination of the two:

$$\rho = -p = \begin{cases} 0 & \text{for } r > r_S \\ \Delta & \text{for } r < r_S \end{cases} \quad (\text{D.1})$$

where $\Delta > 0$. To recover the BH.SW solution outside, we use $V_0 = \Lambda = 0$. The solution to EFE in Eq.B.3 for Eq.D.1 (which we called BH.fv) is then:

$$2\Phi = 2\Psi = \begin{cases} -r_S/r & \text{for } r > r_S \equiv 2GM \\ -r^2 H_\Lambda^2 & \text{for } r < r_S = r_\Lambda \equiv 1/H_\Lambda \end{cases} \quad (\text{D.2})$$

where: $\rho_\Lambda = \rho_{BH} = \Delta$ and $M = \frac{4\pi}{3} r_S^3 \Delta$. Recall that $\Lambda = V_0 = 0$ and ρ_Λ refers to the effective Λ density inside the BH. In a more realistic situation, on larger scales the BH.SW metric should be considered a perturbation of FLRW background, e.g. Eq.16,

with $\Lambda \neq 0$ and $V_0 \neq 0$ (see Appendix E). The above solution has no singularity at $r = 0$. Note how, contrary to what happens in the BH.SW, in the BH.fv solution, the metric components don't change signature as we cross inside r_S . In both sides of r_S we have constant but different values of p and ρ . This comes from energy conservation in Eq.B.4. There is a discontinuity at $2\Phi = -1$ where $r = r_S$, in agreement with Eq.B.4, but the metric is static and continuous at r_S . This solution only happens when $r_S = (8\pi G\Delta/3)^{-1/2}$. The smaller Δ the larger and more massive the BH. In the limit $\Delta \Rightarrow 0$, we have $r_S \Rightarrow \infty$ and we recover Minkowski space, as expected.

This is a well known solution for a BH interior [66, 14]. Is this solution stable (as defined [9])? According to [67] this model is dynamically unstable. In the language of [66], we need $dp/dr = 0$ in the boundary, which requires $p = -\rho = 0$. We will understand the BH.fv solution here as an asymptotic solution for the BH.u model in §3.2 which avoids these discontinuities.

At a fixed location, the scalar field φ inside the BH is trapped in a stable configuration ($\rho = V_0 + \Delta$) and can not evolve ($K = 0$ in Eq.A.3). The same happens for the field outside (see Fig.A.5). A FV in Eq.D.1 with equal Δ but with smaller initial radius $r = R < r_S$ is subject to a pressure discontinuity at $r = R$ which is not balanced in Eq.B.4 and results in a bubble growth [5, 7]. Such boundary grows and asymptotically reaches $R = r_S$ (see top panel of Fig.2). The inside of r_S is causally disconnected, so the pressure discontinuity does not act on $r = r_S$, which corresponds to a trapped surface.

Appendix E. Non empty solution

Eq.D.1 for $V_0 \neq 0$ and $\Lambda \neq 0$:

$$\rho(r) = \begin{cases} V_0 & \text{for } r > r_S \\ V_0 + \Delta & \text{for } r < r_S \end{cases} \quad (\text{E.1})$$

can be solved as $\Phi = \Psi$ with

$$2\Phi = \begin{cases} -r_S/r - r^2 H_{\Lambda_+}^2 & \text{for } r > r_S \equiv 2GM(1 + \epsilon) \\ -r^2 H_{\Lambda_-}^2 & \text{for } r < r_S = r_{\Lambda_-} \equiv 1/H_{\Lambda_-} \end{cases} \quad (\text{E.2})$$

where $\epsilon \equiv \rho_{\Lambda_+}/\Delta$ and

$$3H_{\Lambda_+}^2 \equiv 8\pi G\rho_{\Lambda_+} \quad ; \quad \rho_{\Lambda_+} = \Lambda/8\pi G + V_0 \quad (\text{E.3})$$

$$3H_{\Lambda_-}^2 \equiv 8\pi G\rho_{\Lambda_-} \quad ; \quad \rho_{\Lambda_-} = \rho_{\Lambda_+} + \Delta \quad (\text{E.4})$$

So there are different effective ρ_Λ outside (ρ_{Λ_+}) and inside (ρ_{Λ_-}), but only one Λ . The exterior of the BH has the dSW metric but more generally it is a perturbation of the FLRW metric.

Appendix F. Junction conditions

We can arrive at the same BHU (BH.fv and BH.u) solutions using Israel's junction conditions [68, 69]. We will combine two solutions to EFE with different energy content, as in Eq.21, on two sides (V_4^- and V_4^+) of a hypersurface junction $\Sigma = V_4^- \cap V_4^+$. The inside g^- is FLRW metric and the outside g^+ is BH.SW metric. The junction conditions require that the metric

and its derivative (the extrinsic curvature K) match at Σ . This means that the join metric provides a new solution to EFE in $V_4 = V_4^- [< \Sigma] \cup V_4^+ [> \Sigma]$. In many cases, like in the Bubble Universes, this does not work and the junction requires a surface term (the bubble) to glue both solutions together. We will show that for both timelike and null geodesics the junction conditions are satisfied for the BHU and there are no surface terms. In this section, we follow closely the notation in §12.5 of [27] with $ds^2 = g_{ab}dx^a dx^b$ where $a = 0, 1, 2, 3$ for the 4D metric and $ds_\Sigma^2 = h_{\alpha\beta}dy^\alpha dy^\beta$ with $\alpha = 0, 1, 2$ for the 3D induced metric: i.e. ds^2 restricted to the Σ hypersurface.

Appendix F.1. Timelike Junction

We start by choosing a timelike Σ fixed in comoving coordinates at some value χ_* . This can be identified with a causal boundary, like the freefall collapse of a star of fixed mass M or the particle horizon of Inflation $\chi_\S = \chi_* = (a_i H_i)^{-1}$, where a_i and H_i are the scale factor and Hubble rate when Inflation begins (see Appendix G). The spherical shell radius follows a radial geodesic trajectory in the FLRW metric. This corresponds to a FLRW cloud of fixed mass M that is expanding or contracting (see also [20] and §12.5 of [27]). The induced 3D metric $h_{\alpha\beta}^-$ for $dy^\alpha = (d\tau, d\delta, d\theta)$ and fixed $\chi = \chi_*$, is:

$$ds_{\Sigma^-}^2 = h_{\alpha\beta}^- dy^\alpha dy^\beta = -d\tau^2 + a^2(\tau)\chi_*^2 d\Omega^2 \quad (\text{F.1})$$

For the outside SW frame, the junction Σ^+ is described by $r = R(\tau)$ and $t = T(\tau)$, where τ is the FLRW comoving time. We then have:

$$dr = \dot{R}d\tau \quad ; \quad dt = \dot{T}d\tau, \quad (\text{F.2})$$

where the dot refers to derivatives with respect to τ . The metric h^+ induced in the outside SW metric is:

$$\begin{aligned} ds_{\Sigma^+}^2 &= h_{\alpha\beta}^+ dy^\alpha dy^\beta = -Fdt^2 + \frac{dr^2}{F} + r^2 d\Omega^2 \\ &= -(F\dot{T}^2 - \dot{R}^2/F)d\tau^2 + R^2 d\Omega^2 \end{aligned} \quad (\text{F.3})$$

where $F \equiv 1 - r_S/R$. Comparing Eq.F.1 with Eq.F.3, the first matching conditions $h^- = h^+$ are then:

$$R(\tau) = a(\tau)\chi_* \quad ; \quad F\dot{T} = \sqrt{\dot{R}^2 + F} \equiv \beta(R, \dot{R}) \quad (\text{F.4})$$

For any given $a(\tau)$ and χ_* we can find both $R(\tau)$ and $\beta(\tau)$. We also want the derivative of the metric to be continuous at Σ . For this, we estimate the extrinsic curvature K^\pm normal to Σ^\pm from each side of the hypersurface as:

$$K_{\alpha\beta} = -[\partial_a n_b - n_c \Gamma_{ab}^c] e_\alpha^a e_\beta^b \quad (\text{F.5})$$

where $e_\alpha^a = \partial x^a / \partial y^\alpha$ and n_a is the 4D vector normal to Σ . The outward 4D velocity is $u^a = e_\tau^a = (1, 0, 0, 0)$ and the normal to Σ^- on the inside is then $n^- = (0, a, 0, 0)$. On the outside $u^a = (\dot{T}, \dot{R}, 0, 0)$ and $n^+ = (-\dot{R}, \dot{T}, 0, 0)$. It is straightforward to verify that: $n_a u^a = 0$ and $n_a n^a = +1$ (for a timelike surface) for both n^- and n^+ .

We then find that the extrinsic curvature in Eq.F.5 to the Σ junction, estimated with the inside FLRW metric, i.e. K^- is:

$$\begin{aligned} K_{\tau\tau}^- &= -(\partial_\tau n_\tau^- - a\Gamma_{\tau\tau}^\chi)e_\tau^\tau e_\tau^\tau = 0 \\ K_{\theta\theta}^- &= a\Gamma_{\theta\theta}^\chi e_\theta^\theta e_\theta^\theta = -a\chi_* = -R \end{aligned} \quad (\text{F.6})$$

where we have used Eq.F.4 and the following Christoffel symbols for the FLRW:

$$\begin{aligned} \Gamma_{\tau\tau}^\tau &= \Gamma_{\tau\chi}^\tau = \Gamma_{\tau\tau}^\chi = \Gamma_{\chi\chi}^\chi = 0 \quad ; \quad \Gamma_{\theta\theta}^\tau = a^2\chi_*^2 H \\ \Gamma_{\tau\chi}^\chi &= \Gamma_{\chi\chi}^\tau a^{-2} = H \quad ; \quad \Gamma_{\theta\theta}^\chi = -\chi_* \end{aligned} \quad (\text{F.7})$$

For the SW metric:

$$\begin{aligned} \Gamma_{tt}^t &= \Gamma_{tr}^r = 0 \quad ; \quad \Gamma_{\theta\theta}^r = -FR; \\ \Gamma_{tr}^t &= -\Gamma_{rr}^r = \Gamma_{tt}^r F^{-2} = \frac{r_S}{2FR^2} \end{aligned} \quad (\text{F.8})$$

which results in K^+ :

$$\begin{aligned} K_{\tau\tau}^+ &= \ddot{R}\dot{T} - \dot{R}\ddot{T} + \frac{\dot{T}r_S}{2R^2F}(\dot{T}^2F^2 - 3\dot{R}^2) = \frac{\dot{\beta}}{\dot{R}} \\ K_{\theta\theta}^+ &= \dot{T}\Gamma_{\theta\theta}^r = -\dot{T}FR = -\beta R \end{aligned} \quad (\text{F.9})$$

where we have used the definition of β in Eq.F.4. In both cases $K_{\delta\delta} = \sin^2\theta K_{\theta\theta}$, so that when $K_{\theta\theta}^- = K_{\theta\theta}^+$ it follows that $K_{\delta\delta}^- = K_{\delta\delta}^+$. Comparing Eq.F.6 with Eq.F.9, the matching conditions $K_{\alpha\beta}^- = K_{\alpha\beta}^+$ require $\beta = 1$, which using Eq.F.4 gives:

$$R = [r_H^2 r_S]^{1/3} \quad (\text{F.10})$$

This reproduces the junction in Eq.23. The time equation is:

$$\dot{T} = \frac{1}{1 - R^2 H^2} \quad (\text{F.11})$$

which is the generalization of Eq.20 for $\dot{H} \neq 0$ and agrees with $\partial_\tau t = (1 + 2\Phi_W)^{-1}$ in Eq.17 for $2\Phi_W = -H^2 R^2$, so it corresponds to a time dilation in the comoving frame.

For constant r_S the timelike Σ , only works for a dust ($p = 0$) matter dominated FLRW metric $r_H^2 \propto a^3$, for only in this case Eq.F.10 agrees with $R = a\chi_*$ with a constant χ_* . This corresponds to a FLRW dust cloud of fix mass M expanding or collapsing. This case illustrates well the point we want to make. For $p \neq 0$ we need to consider a null junction, which allows for a general $H(\tau)$, see Eq.25 and Appendix F.3.

Appendix F.2. The GHY boundary term

The expansion inside an isolated BH is bounded by the event horizon $r < r_S$ and we need to add the GHY boundary term S_{GHY} to the action in Eq.6, where:

$$S_{GHY} = \frac{1}{8\pi G} \oint_{\partial V_4} d^3y \sqrt{-h} K \quad (\text{F.12})$$

The integral is over the induced metric at ∂V_4 , which corresponds to Eq.F.1, i.e. $\partial V_4 = \Sigma$ at $R = r_S$:

$$ds_{\partial V_4}^2 = h_{\alpha\beta} dy^\alpha dy^\beta = -d\tau^2 + r_S^2 d\Omega^2 \quad (\text{F.13})$$

So the only remaining degrees of freedom in the action are time τ and the angular coordinates. We can use this metric and Eq.F.6 to estimate K :

$$K = K_\alpha^\alpha = \frac{K_{\theta\theta}}{R^2} + \frac{K_{\delta\delta}}{R^2 \sin^2\theta} = -\frac{2}{R} = -\frac{2}{r_S} \quad (\text{F.14})$$

We then have

$$S_{GHY} = \frac{1}{8\pi G} \int d\tau 4\pi r_S^2 K = -\frac{r_S}{G} \tau \quad (\text{F.15})$$

The Λ contribution to the action in Eq.6 is:

$$S_\Lambda = -\frac{\Lambda}{8\pi G} V_4 = -\frac{r_S^3 \Lambda}{3G} \tau \quad (\text{F.16})$$

We have estimated the total 4D volume V_4 as that bounded by ∂V_4 inside $r < r_S$: $V_4 = 2V_3\tau$, where the factor 2 accounts for the fact that $V_3 = 4\pi r_S^3/3$ is covered twice, first during collapse and again during expansion. Comparing the two terms we can see that we need $\Lambda = 3r_S^{-2}$ or equivalently $r_\Lambda = r_S$ to cancel the boundary term. In other words: evolution inside a BH event horizon induces a Λ term in the EFE even when there is no Λ term to start with. Such event horizon is only a boundary for outgoing geodesics, i.e. expanding solutions. This provides a fundamental interpretation to the observed Λ as a causal boundary [40, 34].

If the BHU also contains a true Λ , FV or DE with constant $\rho = \Delta$, the resulting ρ_Λ and the SW radius r_S are

$$8\pi G \rho_\Lambda = 3r_M^{-2} + \Delta \quad ; \quad r_S = r_\Lambda = \frac{r_M r_\Delta}{(r_M^2 + r_\Delta^2)^{1/2}} \quad (\text{F.17})$$

where $r_M = 2GM$ and $r_\Delta = \sqrt{3\Delta/8\pi G}$. In the limit of $\Delta = 0$ we have $r_S = r_M$. For Δ larger than the BH mass density we have $r_S \simeq r_\Delta$. This is similar BH.fv with some subdominant matter and/or radiation inside. The most general BHU would be a combination of both M and Δ .

Appendix F.3. Null Junction

A null junction has degeneracies which requires more elaborate consideration. This level of detail is beyond the scope of this paper, so we only give a brief account of such calculation. For a more careful analysis see [69]. We choose Σ to be a radial null surface in the FLRW metric, i.e.: $d\tau = ad\chi$. This results in a radial coordinate $\chi_*(\tau)$ which is no longer constant and that we want to identify with the FLRW event horizon of Eq.12. At any given time the corresponding physical distance is $r_*(\tau) = a(\tau)\chi_*(\tau)$ with $\dot{\chi}_* = 1/a$. For the outside SW coordinate system, Σ^+ is described as before by Eq.F.2. The induced inside metric h^- with $y^\alpha = (\tau, \theta, \delta)$ and $d\tau = ad\chi$ is now:

$$h_{\alpha\beta}^- dy^\alpha dy^\beta = a^2 \chi_*^2 d\Omega^2 = r_*^2(\tau) [d\theta^2 + \sin^2(\theta) d\delta^2] \quad (\text{F.18})$$

This has to agree with h^+ in Eq.F.3. The first matching conditions $h^- = h^+$ are in this case:

$$R = r_*(\tau) = a\chi_* \quad \Rightarrow \quad \dot{R} = 1 + HR \quad (\text{F.19})$$

$$F^2 \dot{T}^2 = \dot{R}^2 \quad \Rightarrow \quad \dot{T} = \frac{\dot{R}}{1 - r_S/R} \quad (\text{F.20})$$

The outward 4D velocity is $u^a = e_t^a = (1, 1/a, 0, 0)$, so it has a radial component in the comoving frame. For a null surface we define a transverse extrinsic curvature [69]. We use the same notation as in Eq.F.5 with the difference that n is now a transverse null vector: $n_a u^a = 0$ and $n_a n^a = 0$. We then have: $n^- = A(1, -a, 0, 0)$ where $A = A(\tau)$ is an arbitrary function of τ . On the outside $u^a = (\dot{T}, \dot{R}, 0, 0)$ and $n^+ = (-\dot{R}, \dot{T}, 0, 0)$ as before, but where we have now used the new matching condition above $\dot{R} = F\dot{T}$ in Eq.F.20. Using the Christoffel symbols in Eq.F.7 and Eq.F.8, we find:

$$\begin{aligned} K_{\tau\tau}^- &= -\partial_\tau n_\tau^- - 2A\Gamma_{\tau\chi}^\chi - \frac{1}{a}\partial_\tau n_\chi^- - \frac{A}{a^2}\Gamma_{\chi\chi}^\tau = 0 \\ K_{\tau\tau}^+ &= \ddot{R}\dot{T} - \dot{R}\ddot{T} + \frac{\dot{T}r_S}{2R^2F}(\dot{T}^2F^2 - 3\dot{R}^2) = 0 \\ K_{\theta\theta}^- &= A\Gamma_{\theta\theta}^\tau - aA\Gamma_{\theta\theta}^\chi = AR(HR - 1) \\ K_{\theta\theta}^+ &= \dot{T}\Gamma_{\theta\theta}^r = -\dot{T}FR = -\dot{R}R \\ K_{\delta\delta}^\pm &= \sin^2\theta K_{\theta\theta}^\pm \end{aligned} \quad (\text{F.21})$$

Thus, the second matching conditions $K_{\alpha\beta}^- = K_{\alpha\beta}^+$ together with Eq.F.19 results in:

$$\dot{R} = 1 + HR \quad ; \quad A = \frac{1 + HR}{1 - HR} \quad (\text{F.22})$$

The left hand side is fulfilled for any $H(\tau)$ as long as $R = a\chi_*$ is a null geodesic (i.e. $\chi_* = 1/a$), which is our starting point in Eq.F.19 and agrees with Eq.25 for $V_0 = 1$. The right hand side fixes the normalization $A = A(\tau)$ of n^- in Σ^- .

When a is small the null geodesics $R = r_*$ in the integral of Eq.12 is dominated by the late time value of H_Λ and this means that the FLRW event horizon χ_* is fixed in comoving coordinates. This reproduces the junction in Eq.F.10. On the opposite limit, when H is constant: $H = H_\Lambda = r_\Lambda^{-1}$ we have $\dot{R} = 0$ and $R = r_\Lambda = r_H = r_S$. This results in $2\Psi = 2\Phi = -H^2R^2 = -r_S/R = -1$ in the junction Σ , as in the BH.fv solution of Eq.D.2. This makes sense because for a dS expansion null events are fixed in physical coordinates.

We estimate the GHY boundary term to the action S_{GHY} following the steps in Appendix F.2. We use the formalism in [70] for boundaries of null surfaces. This is similar to what we did before with the difference that the induced metric is now 2D instead of 3D:

$$ds^2 = q_{AB}dz^A dz^B = R^2(d^2\theta + \sin^2\theta d\delta^2) \quad (\text{F.23})$$

$$S_{GHY} = \frac{1}{8\pi G} \oint_{\partial V_4} d\lambda d^2z_\perp \sqrt{q} (\Theta + \kappa) \quad (\text{F.24})$$

where κ is the non-affinity coefficient: $l^a \nabla_a l_b = \kappa l_b$ and $\Theta \equiv q^{AB} \Theta_{AB} = \frac{K_{\theta\theta}}{R^2} + \frac{K_{\delta\delta}}{R^2 \sin^2\theta}$. We can use Eq.F.21 to find $\Theta = -2\dot{R}/R = -2\kappa$. So the corresponding trace of the extrinsic curvature is:

$$\Theta + \kappa = -\frac{\dot{R}}{R} \quad (\text{F.25})$$

For ∂V_4 we have $R = r_S$ and $\dot{R} = 2$. Thus, we recover the same result as Eq.F.14. From this we can arrive to the same conclusion that the boundary GHY term fixes $r_\Lambda = r_S$.

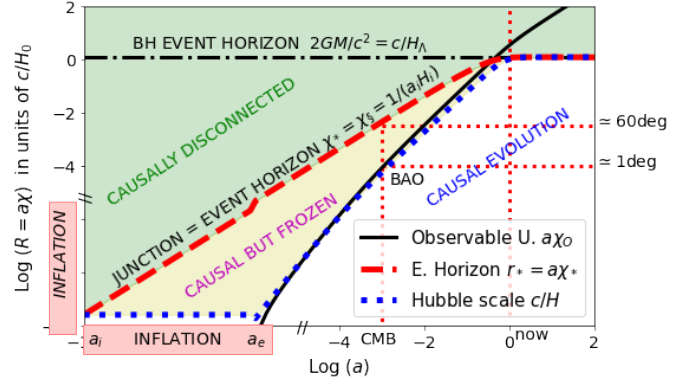


Figure G.7: Extension of Fig.1 to the period of inflation. The FLRW Event Horizon $r_* = a\chi_*$ in Eq.12 (red dashed line) here is also the BHU junction and matches the primordial causal boundary for inflation $\chi_* = \chi_\S$. Scales larger than r_* are causally disconnected (green shading). Our event horizon today $a\chi_* \simeq c/H_\Lambda$ becomes the BH event horizon (dot-dashed line) in the SW frame.

Appendix G. Forming a BHU in an expanding background

To form a BHU during an explosion or rapid expansion we need a FV, ρ_Λ , term as explained in §Appendix A. This will play the role of Dark Energy (DE). Consider a localized field with some fixed total energy $\rho = K + V$ (black dot labeled ρ_5 in Fig.A.5). In an expanding background (such a supernovae explosion or Inflation) the field can rapidly lose its kinetic energy (K_5), due to Hubble damping, and end up trapped inside some FV (V_5). If the outside background is at a lower FV, this will generate an expanding BH of type BH.fv, as discussed in §Appendix D. This could be the start of some inflation. Because additional FV structure can exist within a given FV, the same Hubble damping can form a BH.fv inside a larger BH.fv. When K is not fully damped, the classical reheating mechanism around a FV could also be a source of matter/radiation. This could turn a BH.fv into BH.u (see §3.2). There is some literature on Bubble Universe formation (e.g. see [71, 12] and references therein) but they typically involve quantum gravity ideas or GR extensions. As illustrated in Fig.A.5 there could be a landscape of nested BHU of different masses and sizes. The masses and sizes of such BH.fv bares no relation with the energy of the expansion (e.g. supernova explosion or inflation) or the host object which originated the expansion. Such BHUs are similar to primordial BHs [72].

A possible evolution of our universe is shown in Fig.G.7. The Hubble Horizon r_H is defined as $r_H = c/H$. Scales larger than r_H cannot evolve because the time a perturbation takes to travel that distance is larger than the expansion time. This means that $r > r_H$ scales are "frozen out" (structure can not evolve) and are causally disconnected from the rest (e.g. see [54]). Thus, c/H represents a dynamical causal horizon that is evolving. This was illustrated in Fig.1 and Fig.??.

A primordial field φ settles or fluctuates into a false (or slow rolling) vacuum which will create a BH.fv with null junction Σ in Eq.F.19. Such causal boundary to the particle horizon during inflation $\chi_\S = c/(a_i H_i)$ and the Hubble horizon when inflation begins. The size $R = a(\tau)\chi_\S$ of this vacuum grows

and asymptotically tends to $r_H = c/H$ with $H = H_i$. The inside of this BH will be expanding exponentially $a = e^{\tau H_i}$ while the Hubble horizon is fixed $1/H_i$. According to standard models of primordial inflation [49, 50, 51, 52], this inflation ends (at some a_e) and vacuum energy excess converts into matter and radiation (reheating). This results in BH.u, where the infinitesimal Hubble horizon starts to grow following the standard BB evolution. Note that the inflation in the BH.fv solution stops naturally at cosmic time $\tau_i = -H_i^{-1} \ln \chi_\S H_i$ (see Fig.2) when physical SW distance is $r = a(\tau)\chi_\S = 1/H_i$. In standard models of primordial inflation, H_i is much larger than H_Λ so that $1/H_i$ is much smaller than $1/H_\Lambda$. So a FV Δ only grows to a maximum size $R = r_S = (8\pi G\Delta/2)^{-1/2} = 1/H_i$. Something else has to happen if we want the size to become cosmological. In inflation this is provided by slow rolling. Regardless of these formation details, χ_\S remains the causal scale for the original BH.fv inflation, unless slow rolling ends before. So we propose to identify χ_* in Eq.F.19 with χ_\S from inflation (see also Fig.1) which is equivalent to say that DE is just inflation.

Smaller primordial BH could be created following similar scenarios within the expansion caused by Cosmic Inflation or during a SN explosion. The size of the BHU will depend on the combination of ρ_Λ and the slow rolling mechanism. For such BH.fv it seems that any matter falling inside will be diluted away by the rapid internal expansion and will not affect its size.

References

- [1] R. Penrose, Gravitational collapse and space-time singularities, *Phys. Rev. Lett.* 14 (1965) 57–59.
- [2] J. M. M. Senovilla, Singularity Theorems and Their Consequences, *General Relativity and Gravitation* 30 (5) (1998) 701–848.
- [3] J. M. M. Senovilla, A critical appraisal of the singularity theorems, *Philosophical Transactions of the RS of London Series A* 380 (2222) (2022).
- [4] N. Dadhich, Singularity: Raychaudhuri equation once again, *Pramana* 69 (1) (2007) 23. [arXiv:gr-qc/0702095](#).
- [5] S. K. Blau, E. I. Guendelman, A. H. Guth, Dynamics of false-vacuum bubbles, *PRD* 35 (6) (1987) 1747–1766.
- [6] P. O. Mazur, E. Mottola, Gravitational Condensate Stars: An Alternative to Black Holes, [arXiv e-prints \(2001\) gr-qc/0109035](#).
- [7] A. Aguirre, M. C. Johnson, Dynamics and instability of false vacuum bubbles, *PRD* 72 (10) (2005) 103525.
- [8] H. A. Buchdahl, General relativistic fluid spheres, *Phys. Rev.* 116 (1959) 1027–1034.
- [9] R. Brustein, A. J. M. Medved, Resisting collapse, *PRD* 99 (6) (2019) 064019.
- [10] J. R. Oppenheimer, H. Snyder, On Continued Gravitational Contraction, *Physical Review* 56 (5) (1939) 455–459.
- [11] D. A. Easson, R. H. Brandenberger, Universe generation from black hole interiors, *J. of High Energy Phys.* 2001 (6) (2001) 024.
- [12] N. Oshita, J. Yokoyama, Creation of an inflationary universe out of a black hole, *Physics Letters B* 785 (2018) 197–200.
- [13] R. G. Daghigh, J. I. Kapusta, Y. Hosotani, False Vacuum Black Holes and Universes, [arXiv:gr-qc/0008006](#) (Aug. 2000).
- [14] P. F. Gonzalez-Diaz, The space-time metric inside a black hole., *Nuovo Cimento Lettere* 32 (1981) 161–163.
- [15] D. V. Galtsov, J. P. Lemos, No-go theorem for false vacuum black holes, *Classical and Quantum Gravity* 18 (9) (2001) 1715–1726.
- [16] I. Dymnikova, Spherically Symmetric Space Time with Regular de Sitter Center, *International Journal of Modern Physics D* 12 (6) (2003) 1015–1034.
- [17] R. K. Pathria, The Universe as a Black Hole, *Nature* 240 (5379) (1972) 298–299.
- [18] I. J. Good, Chinese universes, *Physics Today* 25 (7) (1972) 15.
- [19] N. Popławski, Universe in a Black Hole in Einstein-Cartan Gravity, *ApJ* 832 (2) (2016) 96. [arXiv:1410.3881](#).
- [20] W. M. Stuckey, The observable universe inside a black hole, *American Journal of Physics* 62 (9) (1994) 788–795.
- [21] L. Smolin, *The life of the cosmos*, 1997.
- [22] T. X. Zhang, The Principles and Laws of Black Hole Universe, *Journal of Modern Physics* 9 (9) (2018) 1838–1865.
- [23] H. Knutsen, The idea of the universe as a black hole revisited, *Gravitation and Cosmology* 15 (3) (2009) 273–277.
- [24] D. Hilbert, *Die Grundlage der Physik*, Konigl. Gesell. d. Wiss. Göttingen, Math-Phys K 3 (7) (1915) 395–407.
- [25] S. Weinberg, *Gravitation and Cosmology*, John Wiley & Sons, NY, 1972.
- [26] S. Weinberg, *Cosmology*, Oxford University Press, 2008.
- [27] T. Padmanabhan, *Gravitation*, Cambridge Univ. Press, 2010.
- [28] A. Einstein, *Die Grundlage der allgemeinen Relativitätstheorie*, *Annalen der Physik* 354 (7) (1916) 769–822.
- [29] L. D. Landau, E. M. Lifshitz, *The classical theory of fields*, 1971.
- [30] S. M. Carroll, *Spacetime and geometry*. Addison-Wesley., 2004.
- [31] J. W. York, Role of Conformal Three-Geometry in the Dynamics of Gravitation, *PRL* 28 (16) (1972) 1082–1085.
- [32] G. W. Gibbons, S. W. Hawking, Cosmological event horizons, thermodynamics, and particle creation, *PRD* 15 (10) (1977) 2738–2751.
- [33] S. W. Hawking, G. T. Horowitz, The gravitational Hamiltonian, action, entropy and surface terms, *Class Quantum Gravity* 13 (6) (1996) 1487–1498.
- [34] E. Gaztañaga, The cosmological constant as a zero action boundary, *MNRAS* 502 (1) (2021) 436–444.
- [35] J. García-Bellido, L. Espinosa-Portalés, Cosmic acceleration from first principles, *Physics of the Dark Universe* 34 (2021) 100892. [arXiv:2106.16014](#).
- [36] L. Espinosa-Portalés, J. García-Bellido, Covariant formulation of non-equilibrium thermodynamics in General Relativity, *Physics of the Dark Universe* 34 (2021) 100893.
- [37] R. Arjona, L. Espinosa-Portales, J. García-Bellido, S. Nesseris, A GREAT model comparison against the cosmological constant, [arXiv e-prints \(2021\) arXiv:2111.13083](#)[arXiv:2111.13083](#).
- [38] G. F. R. Ellis, T. Rothman, Lost horizons, *American Journal of Physics* 61 (10) (1993) 883–893.
- [39] S. Deser, J. Franklin, Schwarzschild and Birkhoff a la Weyl, *American Journal of Physics* 73 (3) (2005) 261–264. [arXiv:gr-qc/0408067](#).
- [40] E. Gaztañaga, The size of our causal Universe, *MNRAS* 494 (2) (2020) 2766–2772.
- [41] P. Fosalba, E. Gaztañaga, Explaining cosmological anisotropy: evidence for causal horizons from CMB data, *MNRAS* 504 (4) (2021) 5840–5862.
- [42] E. Gaztañaga, P. Fosalba, A peek outside our Universe (2021) [arXiv:2104.00521](#).
- [43] B. Camacho, E. Gaztañaga, A measurement of the scale of homogeneity in the Early Universe, [arXiv e-prints \(2021\) arXiv:2106.14303](#)[arXiv:2106.14303](#).
- [44] K. Lanczos, Bemerkung zur de Sitterschen Welt, *Phys.Z.* 23 (24) (1922) 539–543.
- [45] K. Lanczos, C. Hoenselaers, On a Stationary Cosmology in the Sense of Einstein's Theory of Gravitation [1923], *GR and Gravitation* 29 (1997) 361–399.
- [46] A. Mitra, Interpretational conflicts between the static and non-static forms of the de Sitter metric, *Nature Sci. Reports* 2 (2012) 923.
- [47] V. Faraoni, F. Atieh, Turning a Newtonian analogy for FLRW cosmology into a relativistic problem, *PRD* 102 (4) (2020) 044020.
- [48] E. Gaztañaga, The Cosmological Constant as Event Horizon, *Symmetry* 14 (2) (2022) 300. [arXiv:2202.00641](#).
- [49] A. A. Starobinskiĭ, Spectrum of relict gravitational radiation and the early state of the universe, *Soviet J. of Exp. and Th. Physics Letters* 30 (1979) 682.
- [50] A. H. Guth, Inflationary universe: A possible solution to the horizon and flatness problems, *PRD* 23 (2) (1981) 347–356.
- [51] A. D. Linde, A new inflationary universe scenario, *Physics Letters B* 108 (6) (1982) 389–393.
- [52] A. Albrecht, P. J. Steinhardt, Cosmology for Grand Unified Theories with Radiatively Induced Symmetry Breaking, *PRL* 48 (17) (1982) 1220–1223.
- [53] A. R. Liddle, Observational tests of inflation, [arXiv e-prints \(1999\) astro-ph/9910110](#)[arXiv:astro-ph/9910110](#).

- [54] S. Dodelson, Modern cosmology, Academic Press, NY, 2003.
- [55] E. R. Harrison, Fluctuations at the Threshold of Classical Cosmology, *PRD* 1 (10) (1970) 2726–2730.
- [56] Y. B. Zel'Dovich, Reprint of 1970A&A.....5...84Z. Gravitational instability: an approximate theory for large density perturbations., *AAP* 500 (1970) 13–18.
- [57] P. J. E. Peebles, J. T. Yu, Primeval Adiabatic Perturbation in an Expanding Universe, *ApJ* 162 (1970) 815.
- [58] N. Kaloper, M. Kleban, D. Martin, McVittie's legacy: Black holes in an expanding universe, *PRD* 81 (10) (2010) 104044.
- [59] E. Gaztañaga, How the big bang endup inside a black hole, *Universe Proceedings Alternative Gravities and Fundamental Cosmology* (2) (2022).
- [60] S. Yeung, M.-C. Chu, Directional Variations of Cosmological Parameters from the Planck CMB Data, *arXiv e-prints* (2022) [arXiv:2201.03799](#).
- [61] E. Abdalla, et al, Cosmology Intertwined: A Review of the Particle Physics, Astrophysics, and Cosmology Associated with the Cosmological Tensions and Anomalies, [arXiv:2203.06142](#) (Mar. 2022).
- [62] C. O'Riadaigh, S. Mitton, A new perspective on steady-state cosmology (2015) [arXiv:1506.01651](#).
- [63] H. Bondi, T. Gold, The Steady-State Theory of the Expanding Universe, *MNRAS* 108 (1948) 252.
- [64] F. Hoyle, A New Model for the Expanding Universe, *MNRAS* 108 (1948) 372.
- [65] A. Diez-Tejedor, A. Feinstein, Homogeneous scalar field the wet dark sides of the universe, *PRD* 74 (2) (2006) 023530.
- [66] R. C. Tolman, *Relativity, Thermodynamics, and Cosmology*, 1934.
- [67] Ø. Grøn, H. H. Soleng, Dynamical instability of the González-Díaz black hole model, *Physics Letters A* 138 (3) (1989) 89–94.
- [68] W. Israel, Singular hypersurfaces and thin shells in general relativity, *Nuovo Cimento B Serie* 48 (2) (1967) 463–463.
- [69] C. Barrabès, W. Israel, Thin shells in general relativity and cosmology: The lightlike limit, *PRD* 43 (4) (1991) 1129–1142.
- [70] K. Parattu, S. Chakraborty, B. R. Majhi, T. Padmanabhan, A boundary term for the gravitational action with null boundaries, *General Relativity and Gravitation* 48 (7) (2016) 94. [arXiv:1501.01053](#).
- [71] J. Garriga, A. Vilenkin, J. Zhang, Black holes and the multiverse, *JCAP* 2016 (2) (2016) 064. [arXiv:1512.01819](#).
- [72] A. e. Kusenko, Exploring Primordial Black Holes from the Multiverse with Optical Telescopes, *PRL* 125 (18) (2020) 181304. [arXiv:2001.09160](#).